

INSIGHTS INTO THE MAGNETIC ORIGIN OF Cu_nCr ($n = 9 \div 11$) CLUSTERS: A SUPERPOSITION OF MAGNETIC AND ELECTRONIC SHELLS

Nguyen Thi Mai^{1,2}, Ngo Thi Lan^{1,2,3}, Nguyen Thanh Tung^{1,2,*}

¹Graduate University of Science and Technology, VAST, 18 Hoang Quoc Viet, Ha Noi, Vietnam

²Institute of Materials Science, VAST, 18 Hoang Quoc Viet, Ha Noi, Vietnam

³University of Science, Thai Nguyen University, Tan Thinh, Thai Nguyen City, Thai Nguyen, Vietnam

*Email: tungnt@ims.vast.ac.vn

Received: 6 August 2019; Accepted for publication : 22 October 2019

Abstract. Interests in Cu-Cr sub-nanometer systems have been increasing due to the recently-found icosahedral Cu_{12}Cr cluster as a superatomic molecule, where the 3d-Cr and 4s-Cu electrons can phenomenologically form the 18-e molecular shell ($1S^21P^61D^{10}$) of Cu_{12}Cr . In this report, we set out to investigate the energetically-preferred geometries and stabilities of Cu_nCr ($n = 9 \div 11$) clusters using the density-functional-theory calculations. It is found that not all of 3d-Cr electrons involve in the formation of the cluster shell and the remaining localized ones cause the magnetic moment of the clusters, which is different from what was believed. The calculated molecular diagram, natural orbital analysis, and spin-density computation are performed to elaborate our idea.

Keywords: Copper-chromium clusters, magnetic moment, superatoms, s-d hybridization.

Classification number: 2.2.1, 2.4.1, 4.10.4.

1. INTRODUCTION

In the field of advanced materials science, artificial atomic assemblies with structure sizes below nanometers have recently been of a great interest due to their potential as building blocks for novel nanostructured materials [1-10]. The most fascinating feature of atomic clusters is the anomalous change of their geometric and electronic structures upon adding or removing only a single atom [11]. This interesting property is exploited to create sustainable superatoms with desired functionalities that can replace or outperform existing elements in the Periodic table. In this regard, doping of copper clusters with different atoms is expected to tailor the structural, electronic, catalytic, and magnetic properties for applications in materials science, solid states chemistry, microelectronics and nanotechnology [6-10, 12-20]. For instance, the electronic structure of scandium-doped copper cluster cations Cu_nSc^+ were investigated. The Cu_{17}Sc cluster was found to be a superatomic molecule, Cu_{15}Sc was found to be a stable cluster with a large

dissociation energy and a closed electronic structure, hence this can be regarded as a superatom [21]. The nucleation energy and reactivity descriptors of Cu_nM ($\text{M}=\text{Ni}, \text{Pd}, \text{Pt}; n = 1-4$) bimetallic nanoparticles supported on MgO (111) surface have been studied by density functional theory method and compared to their gas phase counterparts [15]. The magnetic properties of small Cu_nTM clusters ($n = 3-7, 12; \text{TM}=\text{Ru}, \text{Rh}, \text{Pd}$) have been studied. The magnetic of Cu_nTM clusters are mainly affected by symmetry, coordination number and atomic distance [22]. The geometrical, electronic and magnetic properties of small Cu_nFe ($n = 1-12$) clusters have been investigated by using density functional. The Cu_7Fe cluster with a large energy gap (2.61 eV) can be perceived as a superatom [13].

Recently, the investigation on Cu_nCr clusters ($n = 9-16$) has found that Cu_{12}Cr is exceptionally stable and chemically inert as a superatomic molecule [23]. The magnetic moment of Cu_nCr clusters is governed mainly by the interaction between d - s valence orbitals of Cr and Cu atoms [23]. The magnetic moment of Cu_nCr ($n = 9-11$) clusters can be understood by incompleting electronic shell configuration $1\text{S}^21\text{P}^61\text{D}^9$ for Cu_{11}Cr , $1\text{S}^21\text{P}^61\text{D}^8$ for Cu_{10}Cr , and $1\text{S}^21\text{P}^61\text{D}^7$ for Cu_9Cr . In this report, we perform a quantitative analysis on the molecular diagram and cluster-spin density in order to provide a deeper understanding on the magnetism origin of Cu_nCr ($n = 9-11$) clusters.

2. COMPUTATIONAL METHOD

In order to study the Cu_nCr clusters ($n = 9-11$) we use the method of density functional theory (DFT) which is implemented in the Gaussian 09 software [24, 25]. We have recalculated the optimized geometries of Cu_nCr clusters ($n = 9-11$) using the BP86 functional with the basis sets cc-pvTZ-pp for Cu atom and cc-pvTZ for Cr atom to confirm the results presented in Ref. [23]. The previous investigation on ScCu_n clusters also indicated that results obtained by the BP86 functional are well-matched to experimental values [21]. The calculations are followed by frequency calculations to confirm the stationary structures are minimal. The electronic structure of Cu_nCr global minima clusters were explored using the spin multiplicities, spin-density, the molecular orbital diagram and the natural orbital analysis of Cu_nCr clusters.

3. RESULTS AND DISCUSSION

3.1. Optimized structures and spin multiplicities

The most stable optimized structures of the Cu_nCr clusters with $n = 9-11$ are illustrated in Figure 1. Firstly, the Gaussview program has been used to construct all possible structures of pure Cu_n clusters. Then a Cr atom has been added into the stable structures of the Cu_n clusters at different positions forming the Cu_nCr clusters which are the input structures for the next optimization calculations. In the following, we denote each structure as $n.x$, in which n stands for number of Cu atoms in cluster Cu_nCr and x is labeled as A, B, C and D for isomers with increasing order of energy.

Cu_9Cr . A lot of isomers have been found, including some low-energy isomers. In the first isomer quartet 9.A, the Cr atom is encapsulated by a pentagonal pyramid and three Cu atoms. This is the most stable isomer of Cu_9Cr cluster. The quartet 9.B, doublet 9.C, and sextet 9.D have a slightly distorted form of 9.A with 0.43, 0.61 and 0.83 eV less stable than the ground state, respectively.

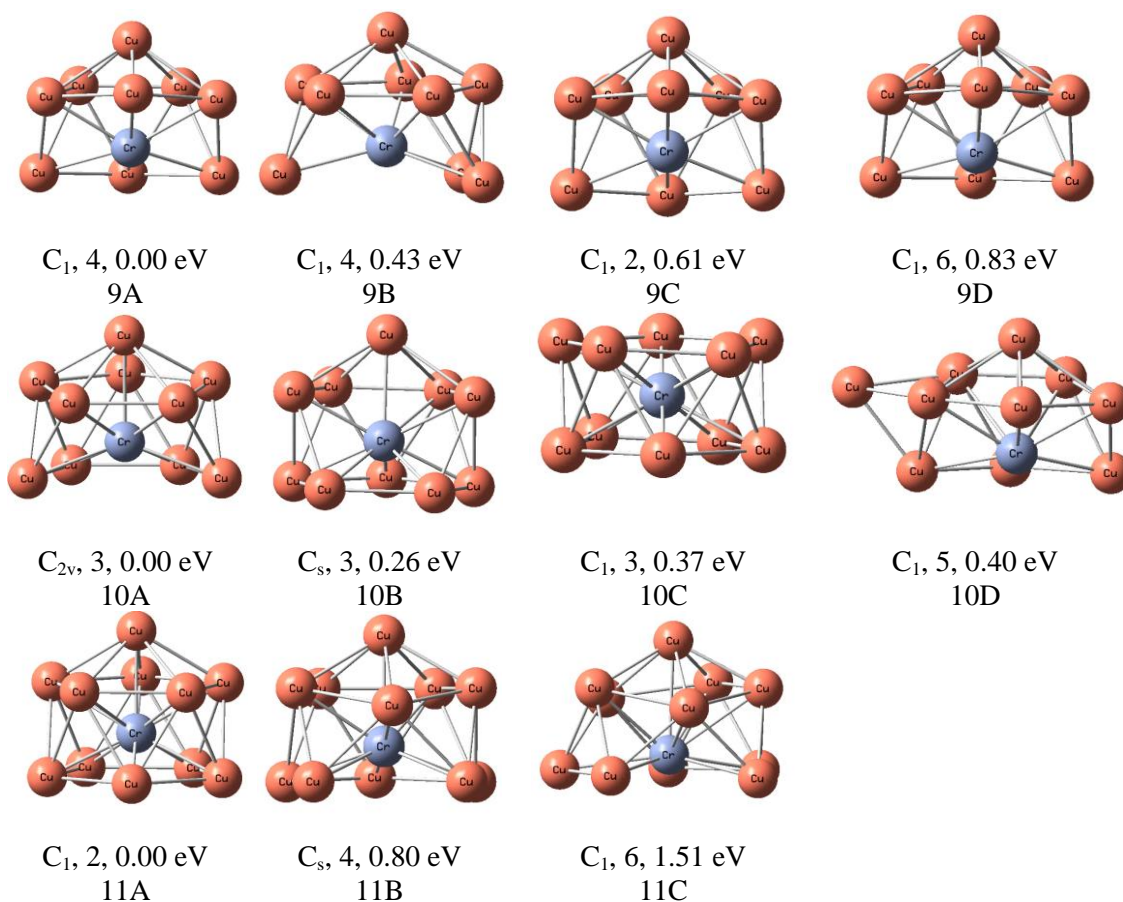


Figure 1. The ground-state structures of Cu_nCr ($n = 9-11$) clusters, and low-lying isomers for Cu_nCr clusters. The point group, spin multiplicity, and energy difference compared to each ground state structure are given. The orange and violet balls represent Cu and Cr atoms, respectively.

Cu_{10}Cr . The triplet 10.A, the Cr atom is surrounded by a pentagonal pyramid and an opened four-member Cu_4 string. With a relative energy of 0.26 eV, the next isomer 10.B is composed of a Cr atom encapsulated by a square pyramid and a five-member Cu_5 ring. The isomer 10.C has an anti-prism form, located at 0.37 eV above the 10.A. Other low-lying energy isomers, the quintet 10.D is unstable with 0.40 eV above the ground state 10.A.

Cu_{11}Cr . The isomer 11.A in which the Cr atom captured by a pentagonal pyramid and a Cu_5 five-member ring is the most stable isomer of Cu_{11}Cr cluster. Two next isomers 11.B and 11.C, having quartet and sextet states with a small distortion in geometry, are highly unstable.

The cluster magnetic states are very stable. For Cu_9Cr , the minimum energy required to switch the spin state (from quartet to doublet) is 0.61 eV. This value is 0.40 eV for Cu_{10}Cr (from triplet to quintet) and 0.80 eV for Cu_{11}Cr (from doublet to quartet) correspondingly.

3.2. Electronic and magnetic properties

In the previous work, the spin states of Cu_nCr ($n = 9-11$) clusters have been well explained by the phenomenological shell [23] in which six outermost valence electrons of Cr atom ($3d^5 4s^1$) and n $4s^1$ valence electrons of Cu atoms are assumed to freely delocalize and jointly form a

molecular shell of the cluster. Taking that picture in mind, the quartet state of Cu_9Cr can be understood in accordance to the particular electronic shell of $1S^21P^61D^7$ with three unpaired electrons. Similar to the cases of Cu_{11}Cr and Cu_{10}Cr , their electronic shell configuration are $1S^21P^61D^9$ and $1S^21P^61D^8$, respectively. In order to quantitatively determine the origin of unquenched magnetic states, we perform the molecular diagram, local magnetic moments (LMM in μ_B), electron configurations of Cr atom and density of state analysis for Cu_nCr ($n = 9-11$) clusters. The results are shown in Fig. 2 and Table 1.

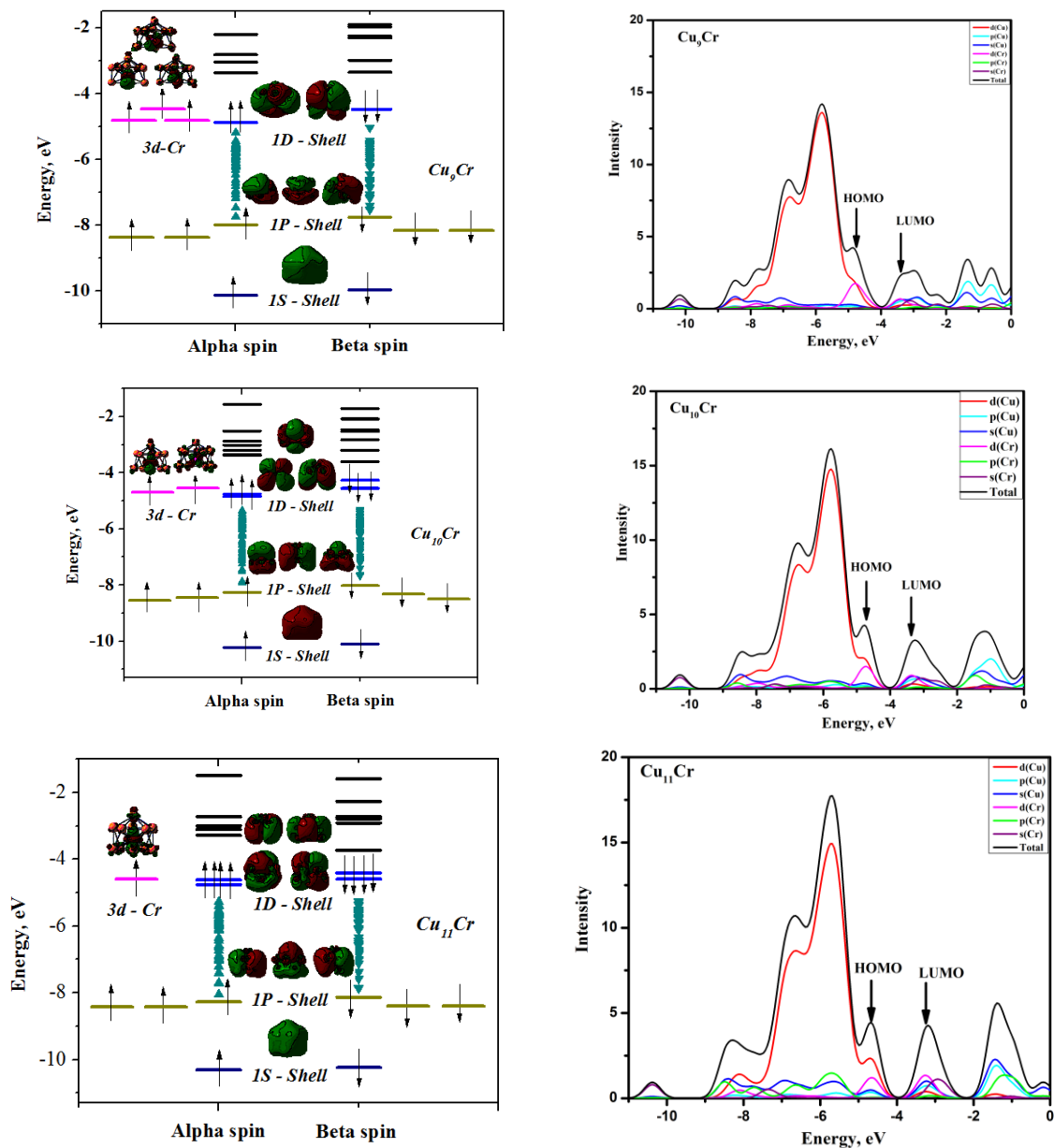


Figure 2. Total/partial DOS (right) and the molecular diagrams (left) of Cu_nCr ($n = 9-11$) clusters are calculated at BP86/cc-pvTZ, cc-pvTZ-pp level of theory. The corresponding shapes of HOMO–LUMO are presented.

Table 1. Electron Configurations Cr atom and Local Magnetic Moments (LMM in μ_B).

n	Electron Configurations Cr atom		LMM(Cr)			LMM(Cu _n)		
	α -spin orbital	β -spin orbital	4s	4p	3d	4s	4p	3d
9	[core]4s ^{0.28} 3d ^{4.62} 4p ^{0.77} 5d ^{0.06}	[core]4s ^{0.21} 3d ^{1.43} 4p ^{0.69} 5d ^{0.04}	0.1	0.0	3.2	-0.4	-0.2	0.2
10	[core]4s ^{0.26} 3d ^{4.57} 4p ^{0.98} 5d ^{0.06}	[core]4s ^{0.23} 3d ^{2.15} 4p ^{0.91} 5d ^{0.04}	0.0	0.0	2.4	-0.5	-0.3	0.2
11	[core]4s ^{0.25} 3d ^{4.47} 4p ^{1.19} 5d ^{0.03}	[core]4s ^{0.24} 3d ^{3.15} 4p ^{1.15} 5d ^{0.01}	0.0	0.0	1.4	-0.4	-0.3	0.2

The results show that for both alpha and beta spin orbitals of Cr atom the occupancy of 3d-Cr is major. The local magnetic moment of Cr atom gradually decreases from 3.2 μ_B to 1.4 μ_B and the total magnetic moment of clusters gradually decreases from 3 μ_B to 1 μ_B with increasing the size n from 9 to 11. In this Fig. 2, analyzing the total/partial DOS of n = 9-11 clusters shows that the 3d-Cr orbital contribution in the HOMO peak (at -4.6 eV) of CrCu₉, CrCu₁₀, and CrCu₁₁ clusters are 56.1 %, 53.2 % and 43.2 %, respectively. For all of the investigated ground-state structures, the total magnetic moment of the clusters is largely localized in the Cr atoms, and their unpaired 3d electrons govern the total magnetic moment of the clusters.

It is surprising that the outermost (3d⁵4s¹) valence electrons of Cr atom are not fully hybridized and entirely delocalized to form the molecular shell as expected. The molecular diagrams of all three considered clusters indicate a partial hybridization between 3d-Cr and 4s-Cu electrons and interestingly, the molecular shell of 3d-Cr and 4s-Cu electrons and the atomic shell of 3d-Cr electrons both are coexisting. In particular, the Cr atom donates 3, 4, and 5 valence electrons to the molecular shell of Cu₉, Cu₁₀, and Cu₁₁ to form the electronic configuration 1S²1P⁶1D⁴, 1S²1P⁶1D⁶, and 1S²1P⁶1D⁸, respectively. The remaining 3, 2, and 1 valence electron(s) are localized in the d-orbitals of the Cr atom.

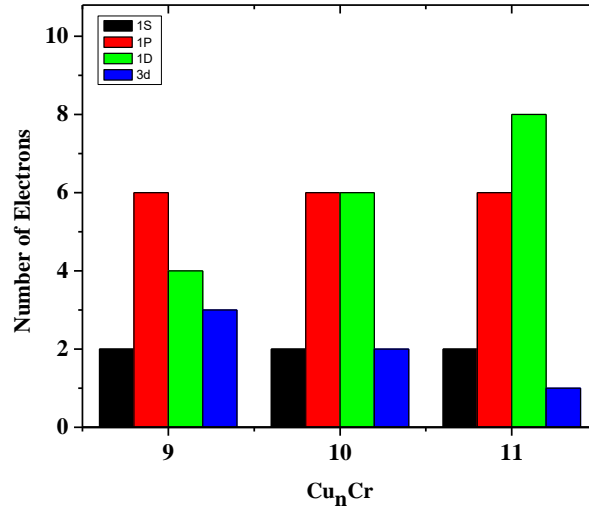


Figure 3. Electronic shell fillings of Cu_nCr (n = 9-11). The black, red and green columns in the electron shell filling diagrams represent the occupation of 1S, 1P and 1D shell, respectively. The occupation of the localized 3d Cr orbitals is given by the blue column.

These localized electrons are unpaired causing the magnetic moment of the clusters while the delocalized electrons in the molecular shell are all paired like those in the pure Cu clusters. It

should be mentioned that the pure Cu clusters show a strong odd-even behavior in which the valence electrons prefer to exist in pairs rather than to fill the molecular orbital following the Hund's rule as seen in individual atoms [26]. There is no singly occupied orbital found in the molecular shell since they are less stable (or require more energy) than the $3d$ -orbital of the Cr atom. This observation is also in a good agreement with the odd-even behavior of pure Cu clusters.

The results from natural orbital analysis are summarized in Fig. 3 where the electronic shell fillings of Cu_nCr ($n = 9-11$) are presented. It can be seen that when n goes from 9 to 11, the interior shells (1S and 1P) of the clusters are unaffected. Nevertheless, the number of electrons in the outer shell (1D) is varied as 4, 6, and 8, respectively, in an agreement with the above observation in molecular diagram. At the same time, the number of localized electrons in $3d$ -Cr orbitals is reduced as 3, 2, and 1, accordingly. The increment of 1D electrons simultaneously comes from $4s$ -Cu orbitals for added Cu atoms and $3d$ -Cr localized orbitals.

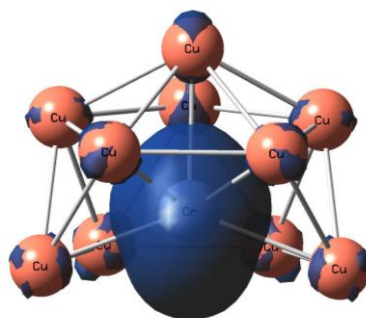


Figure 4. Spin density (blue basin for spin-alpha) of the ground-state Cu_{10}Cr cluster.

As one should be agreed that the Cu_nCr clusters ($n = 9-11$) possess a certain spin states. In the previous work [23], the results went to the same conclusion that the studied clusters exhibit a magnetic moment but the question about their magnetic origin has not been understood completely yet. By knowing where the unpaired electrons locate, in this report we could pre-empt by our physical intuition that the unpaired electrons are on the $3d$ orbitals of Cr atom. This picture can be visualized by plotting the spin distribution of the obtained energy minima structures. As demonstrated in Fig. 4, the total spin mainly locates at the dopant position, in line with the above discussion. The exact electronic configurations of Cu_9Cr , Cu_{10}Cr , and Cu_{11}Cr can be assigned as $1S^21P^61D^43d_{\text{Cr}}^{3\uparrow}$, $1S^21P^61D^63d_{\text{Cr}}^{2\uparrow}$, and $1S^21P^61D^83d_{\text{Cr}}^{1\uparrow}$, respectively.

4. CONCLUSIONS

The method of density functional theory using the BP86 functional and cc-pvTZ, cc-pvTZ-pp basis set have been employed to optimize geometrical structures following by frequency calculations of the clusters Cu_nCr ($n=9-11$). Electronic energies, zero point energies, electron configurations and geometries of the clusters have been derived. The Cu_nCr clusters ($n = 9-11$) possess high spin multiplicities and in this structure there is a superposition of the molecular magnetic shell that form mainly by partial $3d$ -Cr orbitals and the molecular electronic shell composed by partial $3d$ -Cr and all $4s$ -Cu orbitals. We believe that this work will be useful for understanding the physics of magnetic impurities in noble metal clusters and could lead to a rational design of outperforming superatoms with a desired magnetic feature.

Acknowledgements. This work is supported by Institute of Materials Science, Vietnam Academy of Science and Technology.

REFERENCES

1. Claes P., Ngan V. T., Haertelt M., Lyon J. T., Fielicke A., Nguyen M. T., Lievens P., and Janssens E. - The structures of neutral transition metal doped silicon clusters, Si_nX ($n = 6-9$; $\text{X} = \text{V}, \text{Mn}$), *J. Chem. Phys.* **138** (2013) 194301.
2. Tung N. T., Janssens E., and Lievens P. - Dopant dependent stability of Co_nTM^+ ($\text{TM} = \text{Ti}, \text{V}, \text{Cr}, \text{and Mn}$) clusters, *Appl. Phys. B* **114** (2014) 497-502.
3. Tung N. T., Tam N. M., Nguyen M. T., Lievens P., and Janssens E. - Influence of Cr doping on the stability and structure of small cobalt oxide clusters, *J. Chem. Phys.* **141** (2014) 044311.
4. Ngan V. T., Janssens E., Claes P., Lyon J. T., Fielicke A., Nguyen M. T., and Lievens P. - High magnetic moments in manganese-doped silicon clusters, *Chem. Eur. J.* **18** (2012) 15788-15793.
5. Die D., Kuang X. Y., Gua J. J., Zheng B. X. - Density functional theory study of $\text{Au}_n\text{Mn}(n=1-8)$ clusters, *J. Phys. Chem. Solids* **71** (2010) 770-775.
6. Wang H. Q., Kuang X. Y., Li H. F. - Density functional study of structural and electronic properties of bimetallic copper-gold clusters: comparison with pure and doped gold clusters, *Phys. Chem. Chem. Phys.* **12** (2010) 5156-5165.
7. Li G., Wang K., Wang Q., Zhao Y., Du J., He J. - Formation of icosahedral and hcp structures in bimetallic Co-Cu clusters during the freezing processes, *Mater. Lett.* **88** (2012) 126-128.
8. Ma W., Chen F. - Optical and electronic properties of Cu doped Ag clusters, *J. Alloys Compd.* **541** (2012) 79-83.
9. Cheng X. H., Ding D. J., Yu Y. G., Jin M. X. - Geometrical Structures and Electronic Properties of Copper-Doped Aluminum Clusters, *J. Chem. Phys.* **25** (2012) 169-176.
10. Wang L. M., Pal R., Huang W., Zeng X. C., Wang L. S. - Observation of earlier two-to-three dimensional structural transition in gold cluster anions by isoelectronic substitution: MAu_n^- ($n = 8-11$; $M = \text{Ag}, \text{Cu}$), *J. Chem. Phys.* **132** (2010) 114306.
11. Cox D. M., Zakin M. R., and Kaldor A. - Size selective chemical and physical properties of clusters, (1987) US TUA2.
12. Zhou Y. H., Zeng Z., Ju X. - The structural and electronic properties of Cu_mAg_n ($m + n = 6$) clusters, *Microelectron. J.* **40** (2009) 832-834.
13. Wang Ling., Die Dong., Wang Shi-Jian., Zhao Zheng-Quan. - Geometrical, electronic, and magnetic properties of Cu_nFe ($n = 1-12$) clusters: A density functional study, *J. Chem. Phys. Solids* **76** (2015) 10-16.
14. Bagayoko D., Blaha P., Callaway J. - Electronic structure of chromium and manganese impurities in copper, *Phys. Rev.* **34** (1986) 3572-3576.
15. Florez E., Mondragon F., Illas F. - Theoretical study of the structure and reactivity descriptors of Cu_nM ($M = \text{Ni}, \text{Pd}, \text{Pt}$; $n = 1-4$) bimetallic nanoparticles supported on $\text{MgO}(001)$, *Surf. Sci.* **606** (2012) 1010-1018.

16. Jiang Z. Y., Lee K. H., Li S. T., Chu S. Y. - Structures and charge distributions of cationic and neutral Cu_{n-1}Ag clusters ($n = 2-8$), *Phys. Rev. B* **73** (2006) 235423.
17. Bandyopadhyay D. - Architectures, electronic structures, and stabilities of Cu-doped Ge_n clusters: density functional modeling, *J. Mol. Model.* **18** (2012) 3887–3902.
18. Wang J., and Ju-Guang Han - A computational investigation of copper-doped germanium and germanium clusters by the density-functional theory, *J Chem Phys.* **123** (2005) 244303.
19. Ngan V. T., Gruene P., Claes P., Janssens E., Fielicke A., Nguyen M. T., and Lievens P. - Disparate Effects of Cu and V on Structures of Exohedral Transition Metal-Doped Silicon Clusters: A Combined Far-Infrared Spectroscopic and Computational Study *J. Am. Chem. Soc.* **132** (2010) 15589-15602.
20. Mejía-López J., García G., and Romero A. H. - Physical and chemical characterization of $\text{Pt}_{12-n}\text{Cu}_n$ clusters via *ab initio* calculations, *J. Chem. Phys.* **131** (2009) 044701.
21. Veldeman N., Holtzl T., Neukermans S., Veszpremi T., Nguyen M. T., Lievens P. - Experimental observation and computational identification of $\text{Sc}@\text{Cu}^+_{16}$, a stable dopant-encapsulated copper cage, *Phys. Rev. A* **76** (2007) 011201.
22. Sun Q., Gong X. G., Zheng Q. Q., Wang G. H. - First-principles study of the magnetic properties of 4d impurities in Cu_n clusters, *Phys. Lett. A* **209** (1995) 249-253.
23. Pham H. T, Cuong N. T., Tam N. M., and Tung N. T. - A systematic investigation on CrCu_n clusters with $n = 9-16$: Noble gas and tunable magnetic property, *J. Phys. Chem. A* **120** (2016) 7335-7343.
24. Frisch M.J, Schlegel H. B., Scuseria G. E., Robb M. A., Cheeseman J. R, et al., Gaussian 09, Revision A.02, Gaussian, Inc., Wallingford CT, (2009).
25. Hohenberg P., and Kohn W. - Inhomogeneous Electron Gas, *Phys. Rev. B*, **136** (1964) 864.
26. Li C. G., Shen Z. G., Hu Y. F., Tang Y. N., Chen W. G., and Ren B. Z. - Insights into the structures and electronic properties of Cu_{n+1}^{μ} and $\text{Cu}_n\text{S}^{\mu}$ ($n = 1-12$; $\mu = 0, \pm 1$) clusters, *Sci. Rep.* **7** (2017) 1345.